lem resurfaced. At issue then was the first measurements of H_0 by Hubble and Humason (5). Owing to observational uncertainties in the brightnesses of the galaxies and especially to calibration errors in the analysis of the acquired data (from Cepheid variables), they found $H_0 \sim 500$ km s^{-1} Mpc^{-1}. This value meant that $H_0^{-1} \sim 1$ to 2 billion years for the age of the universe, and suddenly the general problem was back: How could Earth be older than the universe?

In turn, this problem gradually faded away as many astronomers (especially Baade) undertook, over decades, better observations and data analyses of the brightnesses and distances of the galaxies. By the 1950s, the value of H_0 had decreased fivefold, and H_0^{-1} had therefore equally lengthened to nearly 10 billion years. Hence, the universe was safely older than Earth, and the age problem went away again, for a while. To be sure, it has resurfaced in more recent years, as noted above. Thus, by the 1980s and into the 1990s, we have the modern version of a recurring age discrepancy: How could some stars within the Milky Way be older than the universe itself? Well, they can't be. It's as simple as that. Something is awry, again.

The most likely outcome is that the current age controversy will simply fade away, just as better observations and improved data analyses caused similar glaring contradictions to evaporate throughout the past century. Indeed, several recent developments favor the dissolution of this problem altogether. For example, today's astronomers (6), even the ones polarized from decades of infighting, seem to be converging on smaller values of H_0, implying that some of us may have been recently underestimating the age of the universe; furthermore, unless more dark matter is actually found, then the universe could be an open one, the further consequence being that the universal age is indeed closer to H_0^{-1}, the upper bound of which, say for $H_0 = 60$ km s^{-1} Mpc^{-1}, would then be in accord with the lower bound of the most ancient stellar ages, namely about 12 billion years. What's more, recent reanalyses of some globular-cluster data [especially enhanced helium abundances, which can raise the brightnesses of such stars (7), and recent results from the Hipparcos satellite, which revise upward the brightnesses of several key variable stars (8)] suggest that the globular clusters might have had their ages overestimated by nearly 20%. If true, then the above-noted average age of 15 billion years for the oldest stars needs to be readjusted to about the 12-billion-year value toward which many current studies seem to be headed.

We need not be overly concerned about the current age controversy, other than to note it as an active area of research that seeks to specify a number (the value of H_0) to an accuracy of better than a factor of 2 when many other cosmologically significant numbers (including those on which it depends, such as the cosmic density) are known only to within a factor of about 10. Frankly, it is remarkable that the ages of the cosmos, stars, and life are so close and that together they seem to be stacking up so well along an ordered arrow of time. As for our cherished notions of cosmic evolution, the subject is hardly affected by this lingering age controversy; the arrow of time itself can be contracted or expanded, a little like an accordion, to match the true age of the universe, whatever it turns out to be. It is the sequence of events along that arrow that is more important than the magnitude of the arrow itself.

References

1. M. Bolte and C. J. Hogan, *Nature* **376**, 399 (1995).
2. B. Chaboyer, P. Demarque, P. J. Kernan, L. M. Krauss, *Science* **271**, 957 (1996).
3. J. D. Birchfield, *The Age of the Earth* (Univ. of Chicago Press, Chicago, 1990).
4. C. Tickell, The Kelvin Lecture, Royal Philosophical Society of Glasgow (28 February 1996).
5. E. P. Hubble, *Proc. Natl. Acad. Sci. U.S.A.* **15**, 168 (1929).
6. A. Sandage *et al.*, *Astrophys. J.* **460**, L15 (1996).
7. A. Sweigart, *ibid.* **474**, L23 (1997).
8. R. M. Catchpole and M. W. Feast, paper presented at "Hipparcos and the H-R Diagram," meeting of the Royal Astronomical Society, London, 14 February 1997.

PROTEIN BIOPHYSICS

Stretching Single Protein Molecules: Titin Is a Weird Spring

Harold P. Erickson

The giant protein titin, which provides most of the elasticity of relaxed striated muscle, can stretch to at least four times its 1-μm resting length. Now, on pages 1109 and 1112 of this issue and in this week's *Nature*, three laboratories report their measurements of the elastic forces generated during stretch and relaxation of single titin molecules (*1*–*3*). They find an exotic mix of entropic springs, sawtooth waves, and hysteresis, unlike the properties of any familiar elastic material. And, at higher forces, we see for the first time what happens when protein domains are unraveled by applied force.

The author is in the Department of Cell Biology, Duke University Medical Center, Durham, NC 27710, USA. E-mail: H.Erickson@cellbio.duke.edu

Titin is primarily a string of 300 immunoglobulin (Ig) and related fibronectin type III (FNIII) repeats (*4*). Each immunoglobulin repeat folds into a globular domain about 2.5 nm in diameter and 4 nm long, producing a filament 1.2 μm in length. It was proposed earlier that stretching titin must unfold the immunoglobulin domains, each domain extending from 4 to 30 nm as it unravels (*5*, *6*). However, the complete sequence revealed a new domain called PEVK (for Pro-Glu-Val-Lys) in the middle of the I-band segment of titin (*4*). Unfolding and straightening this PEVK domain, as well as the partially collapsed immunoglobulin segments, could account for the passive elasticity of skeletal muscle, at least at the forces the muscle usually experiences (*7*). At higher forces, which can occur in extreme stretch and in the stiffer cardiac muscle, immunoglobulin domains too may unravel (*7*, *8*). Now both of these mechanisms are demonstrated in the stretching of single titin molecules.

Two of the groups tethered an individual titin molecule to a plastic bead and used laser tweezers to pull the bead, stretching the titan molecule (*1*, *2*). At lower stretch, force is generated by a mechanism termed here an entropic spring (see figure, upper panel). The entropic spring works because a randomly coiled chain will tend to maximize its configurations as it is buffeted by thermal fluctuations (kT in the figure). A force is required to counteract these thermal forces and extend the chain. Tskhovrebova *et al.* (*1*) resolved two entropic springs in series, one corresponding to the somewhat flexible native immunoglobulin domains and the other to the more flexible denatured PEVK segment.

Kellermayer *et al.* (*2*) fit their data to a single flexible element. The entropic spring provides a very nonlinear force. The force is small, 1 to 2 pN, until ~80% of maximal extension but then rises steeply as the chain is extended beyond 80 to 90% of its maximum length. The entropic spring is somewhat like a leash, exerting a strong force only when maximally extended.

At higher forces, Tskhovrebova *et al.* (*1*) observed the unraveling of immunoglobulin domains. They quickly jerked the bead 250 nm, generating a force of more than 100 pN on the extended titin. Then they observed that the force relaxed in discrete steps, each step extending the chain about 20 nm, close to the prediction for unraveling one immunoglobulin domain (*5*, *6*). The most dramatic demonstration of domain unraveling is in the third study by Rief *et al.* (*3*), who used the atomic force microscope to stretch titin. Their force profile exhibited prominent sawtooth waves, spaced precisely 25 nm apart, as one immunoglobulin domain after another unraveled (see figure, lower panel inset).

All three reports reveal domain unraveling at higher stretch, but each describes a markedly different force required to initiate unraveling, from 20 to 40 pN (*2*), to 100 pN (*1*), to 250 pN (*3*). This discrepancy needs to be sorted out, and when convincing values are obtained, these data from single molecules carefully correlated with measurements from stretching muscle fibers.

The lower panel of the figure illustrates titan's behavior under these high stresses. A ~100-nm length of titin, comprising 25 immunoglobulin domains (five are shown), is stretched between two tethers. When the tethers are very close to each other the titin will be randomly coiled. As the molecule is extended it behaves as an entropic spring; a small force is needed to extend it to **A**. As the titin reaches full extension, the force of the entropic spring increases steeply. At **B** the force is starting to pull out the weakest pair of β strands (arrow). An important conclusion emerging from the new results (*1*–*3*) is that domain unraveling requires a very high force sustained for only a short distance to initiate the process. When the β strands have been displaced ~0.5 nm (*9*), the domain is greatly destabilized, it rapidly unravels (**C**, in figure), and the force drops. As the polypeptide extends, the process is repeated and another domain unravels (**D** to **F**). At this point, the experimenter retracts the tether back toward zero. The force of the entropic spring drops rapidly as the strand collapses into a random coil (**G**). However, even the weak force at **G** prevents the renaturation of the domain. Only when the tether is almost completely retracted (**H**) do the domains start to renature (arrow).

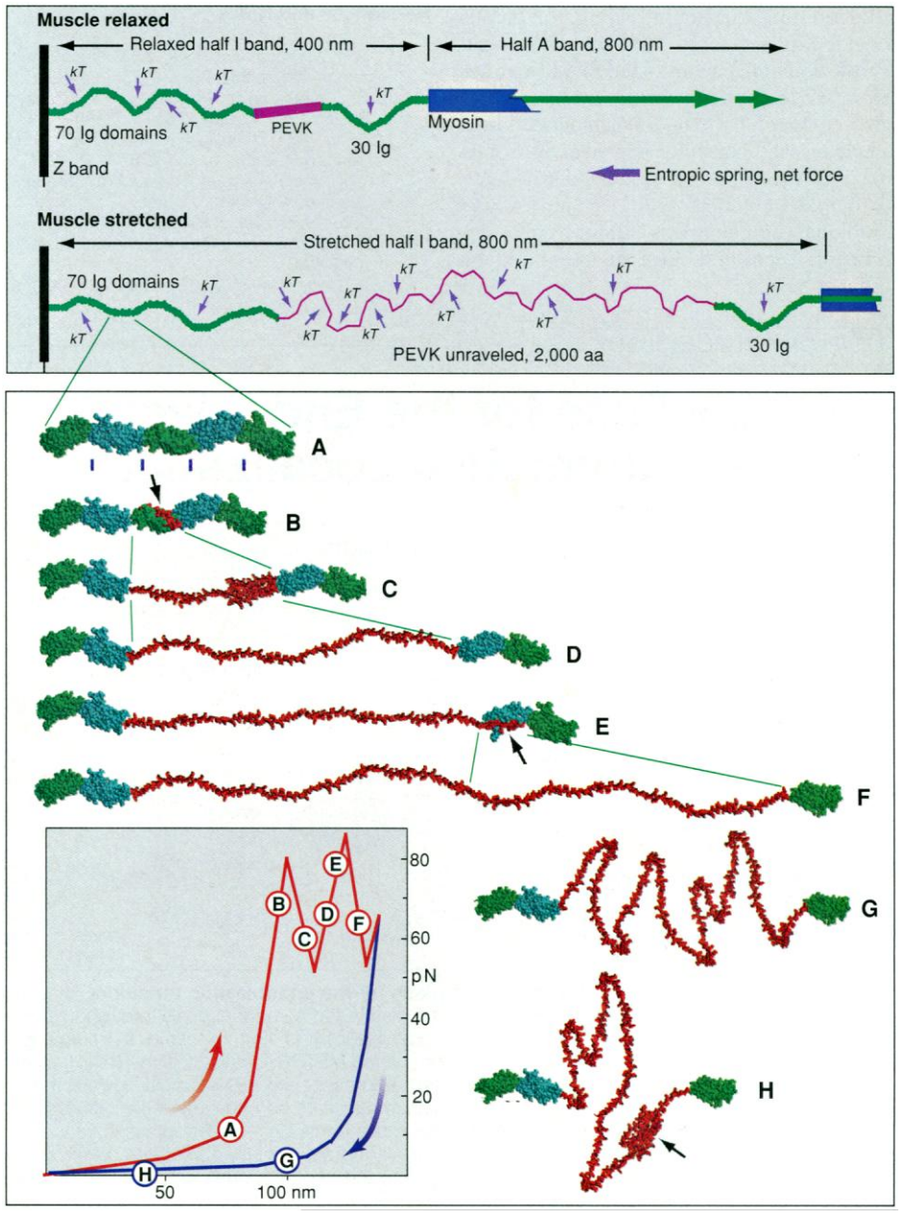

Stretching titan. (**Upper panel**) In a relaxed, unstretched sarcomere the 100 immunoglobulin domains and PEVK domain to the titan I-band segment can span the I band without unfolding. This native titin is flexible and exerts a weak force as an entropic spring. At larger stretch (within physiological range) the PEVK domain unravels and there are then two entropic springs in series: the still-native immunoglobulin segments and the much more flexible extended polypeptide chain of the PEVK. (**Lower panel**) At extreme stretch and higher force, titin immunoglobulin domains unravel one at a time. **A** shows a segment of five folded–immunoglobulin domains colored alternately green and blue, their boundaries indicated by lines. In **C** through **F**, two domains successively unfold to extended polypeptide, which is indicated in red. In **G** the molecule is retracted, exerting a weak force as an entropic spring. Immunoglobulin domains do not refold until the molecule is extensively retracted **H**. The inset plots the force during extension (red line) and retraction (blue line).

The conventional picture of titin is that it operates as a pair of springs on either side of the myosin band, keeping it centered in the sarcomere. This picture now needs rethinking in light of the enormous hysteresis revealed in the new studies, especially when immunoglobulin domains are unfolded. This property is completely unlike a true spring, which is largely reversible. In titin, unfolding immunoglobulin domains may provide a reservoir of extra length in case of extreme stretch. However, there is no obvious way to recover this stretch and refold the domain unless the force is completely relaxed and the stretch retracted. Could chaperones be involved in refolding the immunoglobulin domains after severe stretch?

In summary, the titin I-band segment accommodates physiological stretch by first

straightening, but not unfolding, the immunoglobulin segments, and unfolding the PEVK domain. The unfolded PEVK may act more as a leash than a spring, exerting forces greater than 5 pN (the force generated by a single myosin molecule) only near 80% of its maximal extension. It requires extreme force to unfold immunoglobulin domains. Once unfolded, these domains cannot exert a significant force, and must be renatured by other means.

References and Notes

1. L. Tskhovrebova, J. Trinick, J. A. Sleep, R. M. Simmons, *Nature* **387**, 308 (1997).
2. M. S. Z. Kellermayer, S. B. Smith, H. L. Granzier, C. Bustamante, *Science* **276**, 1112 (1997).
3. M. Rief, M. Gautel, F. Oesterhelt, J. M. Fernandez, H. E. Gaub, *ibid.* **276**, 1109 (1997).
4. S. Labeit and B. Kolmerer, *Science* **270**, 293 (1995).
5. A. Soteriou, A. Clarke, S. Martin, J. Trinick, *Proc. R. Soc. London Ser. B* **254**, 83 (1993).
6. H. P. Erickson, *Proc. Natl. Acad. Sci. U.S.A.* **91**, 10114 (1994).
7. W. A. Linke *et al.*, *J. Mol. Biol.* **261**, 62 (1996); M. Gautel and D. Goulding, *FEBS Lett.* **385**, 11 (1996).
8. H. Granzier, M. Helmes, K. Trombitás, *Biophys. J.* **70**, 430 (1996).
9. A force of 100 pN operating over 0.5 nm corresponds to a free energy of 7 kcal/mol, which is close to the total folding energy of a domain. The implication is that the entire free energy of folding is dissipated by the strong force needed to pull out the first few atoms. In contrast, for refolding, the domain must gather in its full 25 nm or more of polypeptide and compact it into the folded domain. A force of 4 pN operating over 25 nm corresponds to 14 kcal/mol, which is more than sufficient to block refolding. Domain refolding probably cannot occur efficiently until the force is reduced to 1 pN or less.

DEVELOPMENTAL BIOLOGY

A New Face for the Endoplasmic Reticulum: RNA Localization

Laurence D. Etkin

How do you get a perfect sphere to acquire a front and back, right-hand and left-hand sides? Such is the challenge addressed during oogenesis, when the molecular signals that initiate the formation of animal body plan are produced and physically localized in the early oocyte. Much of this information is encoded by localized proteins and RNAs that are organized within distinct regions of the oocyte (*1*). Later on, after fertilization, the developing embryo compartmentalizes and elaborates these early signals to build asymmetries ranging from the simple head versus tail to the complex divergence of right- and left-brain thought processes. How does it all begin?

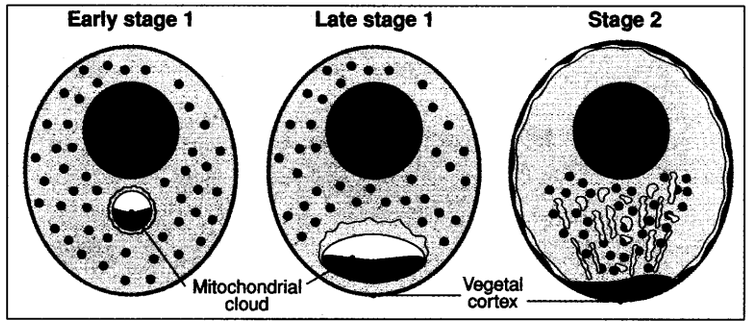

Vg1 put in its place by the endoplasmic reticulum. In early stage 1 oocytes Vg1 mRNA (red) is distributed homogeneously throughout the cytoplasm. The endoplasmic reticulum (yellow) is first detected surrounding the mitochondrial cloud, which contains the METRO-localized RNAs (blue). During late stage 1 the mitochondrial cloud and associated RNAs move toward the vegetal cortex. The endoplasmic reticulum appears on one side of the cloud. In stage 2 oocytes the wedge-shaped structure consisting of endoplasmic reticulum, the colocalizing Vg1 mRNA, and the Vera protein is fully elaborated. Later, during stages 3 and 4, Vg1 will translocate to the vegetal cortex where it will associate tightly with the cortical layer.

In one well-studied oocyte, that of the frog *Xenopus laevis*, the vegetal end of the oocyte contains RNAs that may control germ cell specification and axial patterning. They arrive there by way of two major pathways: the messenger transport organizer (the METRO or early pathway) and the late pathways (*2*, *3*).

The METRO pathway uses a specialized organelle called the mitochondrial cloud to localize RNAs during a very early stage of oogenesis (stage 1). These RNAs include the noncoding repeat Xlsirts, which serves an anchoring function (*4*); the mRNA Xcat2 (*5*); and Xwnt11, which may function in dorsal-ventral patterning (*6*). The second, or late, pathway localizes molecules such as Vg1 (a transforming growth factor–β family member that controls dorsal-ventral patterning) to the vegetal cortex during stages 2 to 4. In this issue, we learn about a surprising new participant in the mechanism by which these pathways function. Deshler *et al.* (page 1128) (*7*) show that Vg1 mRNA is localized via the late pathway by transport through the endoplasmic reticulum, in association with an endoplasmic reticulum–associated protein called Vera (VgLE binding and endoplasmic reticulum association).

In stage 1 and early stage 2 oocytes, while the METRO RNAs are being localized, Vg1 is distributed homogeneously throughout the cytoplasm (*2*, *8*). Then, later in stage 2, Vg1 begins to appear in a wedge-shaped structure associated with the vegetal cortex, at the same site as METRO RNA localization (*2*). During stages 3 and 4, the rest of the Vg1 mRNA is translocated to the cortex in a microtubule-dependent manner. The anchoring of Vg1 at the cortex relies on microfilaments and the noncoding RNA Xlsirts (*9*).

Both cis elements and trans-acting factors help to localize these RNAs. The cis-acting elements responsible for Xlsirts and Xcat2 localization, through the early pathway, are within the Xlsirt 79–nucleotide (nt) repeat sequences (*3*) and the Xcat2 3′ untranslated region (*10*). The translocation of the Vg1 mRNA, through the late pathway, requires a 340- to 366-nt localization element (VgLE) located in its 3′ untranslated region (*11*). A 69-kD microtubule-associated protein binds to the VgLE and may mediate Vg1 interaction with the microtubules in stage 3 oocytes (*12*). Five other proteins (p78, p60, p40, p36, and p33) bind to specific regions of the Vg1 3′ untranslated region, possibly forming part of the translocation complex (*13*).

Deshler *et al.* (*7*) were searching for trans-acting factors that interact with cis-acting elements within the VgLE. They isolated a 75-kD protein, Vera, that interacts specifically with the VgLE region and whose binding to the region is necessary for the proper localization of Vg1 mRNA. Within the VgLE are four elements that, when mutated, interfere with the ability of Vg1 mRNA to localize. Mutations in three of these elements resulted in altered affinity of the 75-kD protein for the VgLE, suggesting that the interaction between the 75-kD protein and these elements is important for the localization of Vg1 mRNA.

The author is in the Department of Molecular Genetics, University of Texas, M. D. Anderson Cancer Center, Houston, TX 77030, USA. E-mail: lde@molgen.mda.uth.tmc.edu